

Supporting Information

Microneedle system with light trigger for precise and programmable penetration

Weijiang Yu†, Jieze Shen†, Chong Ji, Peng Zhang, Hao Chang, Youxiang Wang*, Jian Ji*

1. Experimental Section

Materials: Dopamine hydrochloride, Polycaprolactone (PCL, $M_w = \sim 80000$), acrylamide, N, N'-methylene-bis(acrylamide), and rhodamine 6G (R6G) were supplied by Sigma-Aldrich (Saint Louis, USA). 1-hydroxycyclohexyl phenyl ketone, chitosan (CS, >400 mPa.s) and glutaraldehyde (50%) were obtained from Aladdin (Shanghai, China). Hyaluronate acid (HA, 200kDa~400kDa) was purchased from Bloomage BioTechnology (Jinan, Shandong). Nafion N115 membranes (DuPont, $t = 125$ μm , sulfonic acid form) were purchased from Alfa Aesar (Shanghai, China). Hydrochloric acid and tris (hydroxymethyl) aminomethane were produced by Sinopharm Chemical Reagent (Shanghai, China). Optical cutting temperature compound (O.C.T) was purchased from Sakura Finetek (Torrance, USA). Polydimethylsiloxane (PDMS) Sylgard 184 was purchased from Dow Corning (Rheingaustr, Germany). Adhesive tape was obtained from 3M (Shanghai, China). Stainless steel MN and templates were provided by the Research Institute of Zhejiang University-Taizhou. Porcine organs were purchased from the slaughterhouse. Rabbits were provided by the Zhejiang Academy of Medical Sciences. All animal experiments were carried out strictly according to the "Principles of Laboratory Animal Care" (NIH publication no. 86-23, revised 1985) and have received approval from the Lab Animal Welfare and Research Committee, Zhejiang University.

Fabrication and characterization of Nafion/PDA SMP: Nafion membranes were pre-cleaned sequentially in 3% H_2O_2 at 80°C for 20 min, 0.5 M HCl for 1 h, and then washed with deionized

(DI) water 3 times. All dopamine hydrochloride was used directly. Other reagents such as hydrochloric acid and tris (hydroxymethyl) aminomethane are used without any treatment. Preprocessed Nafion N115 membranes were immersed in dopamine hydrochloride aqueous solution (48 mL, 2.5 mg/mL) for 2 h. Tris buffer solution (12 mL, pH 8.5, 250 mM) was poured in and the concentration of dopamine hydrochloride and Tris buffer were eventually 2 mg/mL and 50 mM, respectively. Nafion membranes were deposited in the solution for 12 h at room temperature. Afterwards, the obtained membranes were immersed in 0.5 M HCl for 1 h for protonation, then treated with deionized water to wash away residual HCl and dried in an oven at 60°C for 20 min. Finally, the obtained Nafion membranes were annealed at 160°C for 20 min to reach their equilibrium states.

The shape memory effect of composite films was proved by the shape recovery cycle under the stress-free condition: In a stress-controlled thermomechanical experiment to evaluate the shape memory effect of PDA-modified Nafion films, the sample was stretched from its initial length (L_0) to a suitable elongation at a temperature above its α transition temperature ($T_{\text{high}} = 150^\circ\text{C}$) and cooled down to T_{low} ($T_{\text{low}} = 25^\circ\text{C}$), which was below its transition temperature range, under constant stress with a cooling rate to generate a final length (L). Afterwards, the sample was unloaded, and equilibrated for 5 min, followed by a temperature ramping from T_{low} to T_{high} in the unloaded mode to recover. Then the sample would be kept at T_{high} for another 20 min.

The relaxation of stress under different recovery temperatures was tested by shape recovery cycle under the iso-strain condition: In a strain-controlled thermomechanical experiment to evaluate the relaxation of the stress of Nafion/PDA films, the sample was stretched from its initial length (L_0) to a stretched length (strain = 100 %) at a temperature above its α transition temperature ($T_{\text{high}} = 100^\circ\text{C}$) and cooled down to T_{low} ($T_{\text{low}} = 25^\circ\text{C}$), which was below its α transition temperature

range, under constant strain with a cooling rate. Afterwards, setting strain to 99.9% to remove stress for 5 min, followed by a temperature ramping to recovery temperature (60, 70, 80, 90, 100°C) in the iso-strain mode. Then the sample would be kept at recovery temperature for another 5 min. The relaxation of stress under different recovery temperatures was shown in **Figure S11**.

Tensile tests were carried out by a universal material testing machine and the strain rate was fixed at 25% min⁻¹ (Z005, Zwick Roell) (**Figure S12**). The photo-thermal conversion capacity of light-responsive SMP was investigated by an 808 nm continuous wave (CW) laser (LSR808H-7W, Lasever Inc., China) and measured using an infrared thermal imaging camera (FLIR E60, Flir System, Inc., USA). The pressing force under different NIR irradiation conditions was tested using a digital balance (**Figure S13**). The effect of the heating rate on the pressing force was carried out by increasing light intensity at rate of 11.2 mW/mm²/s and 11.2 mW/mm²/90s. All the thermomechanical analysis (TMA) experiments were conducted in a tensile mode using a DMA Q800 (TA Instruments, USA).

Shape fixation ratio is to describe the degree of temporary shape fixation. Shape recovery ratio is defined as the recovered strain over the fixed strain. Shape fixation ratio and shape recovery ratio were calculated using the equations (1) and (2) below:

$$\text{shape fixation ratio} = \frac{L_1 - L_0}{L_2 - L_0} \times 100\% \quad (1)$$

$$\text{shape recovery ratio} = \frac{L_3 - L_0}{L_2 - L_0} \times 100\% \quad (2)$$

where L_0 is the original length of the SMP, L_1 is the length of the stretched SMP at deformation temperature, L_2 is the length of the SMP after cooling and load removal, and L_3 is the length of the SMP after recovery.

Fabrication of MN: MN was fabricated via a micromolding approach. PDMS-negative molds were replicated from the stainless-steel MN (tip radius: $\sim 10\ \mu\text{m}$, height: $\sim 1000\ \mu\text{m}$, base width: $\sim 250\ \mu\text{m}$, needle pitch: $\sim 1200\ \mu\text{m}$, basal thickness: $\sim 1000\ \mu\text{m}$, each piece: 3×3 array). To fabricate PCL MN, 0.5 g PCL was placed on the PDMS molds in the vacuum of 0.1 kPa at 125°C for 4 h. After cooling down, these PCL MN were peeled off. R6G was coated on MN by a two-step method. In the first step, the MN was treated with air plasma for 150 s to obtain hydrophilic surfaces. In the second step, 30 μL R6G ethanol solution (0.1 mg/ml) was dropped on the MN by a pipette. To prepare HA MNs, a 0.5 ml solution of 50% (w/v) HA was cast onto PDMS molds. Centrifugation at 5000 rpm for 5 minutes facilitated the filling of the PDMS mold cavities with HA solution. To fabricate crosslinked CS MNs, a 2% (w/v) chitosan solution was prepared by dissolving CS in a 1% (v/v) aqueous solution of acetic acid. The solution was concentrated to 10% (w/v) by evaporating water, and then 0.5 ml of 10% (w/v) chitosan solution containing 1% mol/L glutaraldehyde was filled into the PDMS molds. These MN patches were dried and kept in a desiccator.

Design and fabrication of MSPS: To fabricate MSPS, PCL MN and PDMS film was assembled in the middle of Nafion/PDA film. Both ends of Nafion/PDA films were fixed on the baseplate. The PDMS film was used to prevent PCL MN from melting. To fabricate PDMS films, the mixture of PDMS precursor and curing agent (10:1) was poured on the Petri dishes and then cured in the oven at 90°C for 1 h. After that, the obtained PDMS was cut into square pieces (square piece, side length: 3.0 mm, thickness: 2.0 mm).

In this experiment, the length of SMP film was 2 cm, the height of MSPS was 4 mm, and the distance between the fixed points was 0.9 cm. For the cross-shaped MSPS used in the rabbit

cornea, all ends were fixed on the edge of the tube cylinder adapted from 2 mL and 15 mL centrifuge tubes.

Fabrication of phantom tissues and penetration force measurement: Phantom tissues were fabricated using the crosslinker N¹-Methylene-bis(acrylamide), monomer acrylamide, and initiator 1-hydroxycyclohexyl phenyl ketone. The elastic modulus was regulated by changing the content of the crosslinker and monomer according to published research¹. The precursor solution was polymerized under irradiation of UV light (Intelli-Ray 400, Uvitron, USA) with the intensity of 101.62 mW/mm² at room temperature for 180 s. The elastic modulus of phantom tissues and real tissues was measured by a nanoindenter (tip radius: 44 μm, stiffness: 44.2 N/m. Piuma, Optics, Netherlands) according to our previous research². Seven kinds of phantom tissues were synthesized, and the relative parameters were shown in **Table S3**. The bilayer phantom tissue was fabricated using a two-step curing method (**Figure S14**) with an elastic modulus of 94kPa for the upper layer and an elastic modulus of 194kPa for the underlayer. The underlayer was loaded with 0.1 w/v % methylene blue.

The penetration force measurement of various phantom tissues was performed using R6G coated PCL MN under a continuously increasing force with a precision of 0.02N (**Figure S6**). The force of partial penetration of the needle array was defined as the penetration force.

Light-triggered penetration using MSPSs in vitro and ex vivo: In vitro insertion experiments were performed in phantom tissues. The penetration force produced by MSPS was according to the pressing force-light intensity profile (**Figure 1d** and **Figure S5**) and the penetration force-elastic modulus profile (**Figure 2b**). After NIR irradiation for 120 s, these samples were used for section analysis. Ex vivo experiments were conducted on the porcine liver, intestine, kidney, stomach, and heart. The elastic modulus of porcine tissues was measured (**Table S3**) using a nanoindenter. The

penetration force produced by MSPS was the same as above. After NIR irradiation for 120 s, these samples were collected for histology analysis.

Controllable penetration depth in vitro and in vivo: SMPs with pre-strain of 20%, 30%, 40%, 50%, and 60% were configured in strip-shaped MSPS for in vitro penetration experiments on phantom tissues (94kPa). The initial height of MSPS was 4 mm with $L = 5$ mm, $d = 3$ mm, and $S = 3$ mm. The penetration force of phantom tissue (94kPa) was 0.28 N. According to the stress analysis (**Figure S15a**, $\sin\alpha = 0.6$), the SMP should provide a pressing force of 0.18 N. The shape recovery ratio (R_r) of SMP under 0.18 N was tested as shown in **Figure S9a**. We used the average of R_r to calculate the theoretical penetration depth (light intensity = 14.3 mW/mm²). The actual penetration depth was less than the theoretical penetration depth due to the slowly decreased penetration force during the MN penetration process. As shown in **Figure S15b**, the situation of stress had been changed, the $\sin\beta$ was larger than the $\sin\alpha$ so the penetration force decreased gradually.

The cross-shaped MSPS was used for in vivo penetration of the rabbit cornea, and the MN was attached to the top of the rabbit cornea before irradiation. Other parameters remained unchanged. The penetration force of the rabbit cornea was calculated as 0.74 N according to the method mentioned before. The stress analysis indicated that SMP should provide 0.24 N. The shape recovery ratio (R_r) of SMP was shown in **Figure S9b** under 0.24 N. Thus, the theoretical penetration depth was 158 μ m, 480 μ m, and 606 μ m, respectively. (light intensity = 14.3 mW/mm²).

Patterned penetration and multistage payload delivery: Two stainless steel templates were customized for the fabrication of MSPS unit array: rectangular shape (20 cm \times 6 cm, square pore array: 12 \times 4, spacing: 1.0 cm, pore side length:0.6 cm); square shape (10 cm \times 10 cm, square pore array: 6 \times 6, spacing: 1.0 cm, pore side length:0.6 cm). Cross-shaped MSPS was employed as the

penetration unit. The penetration experiments were performed on phantom tissue with an elastic modulus of 94kPa. R6G coated MN was used to investigate the multistage payload release. To measure the accumulated release of R6G, the applied sites of the phantom tissue were cut and immersed in 10 ml water overnight. Then these solutions were measured by UV-Vis spectrum to calculate the release amount (UV-2550, Shimadzu, Japan)

Histology: Animal tissues and phantom samples were embedded in the OCT compound immediately by a bath of liquid nitrogen. These samples were then cut into 12 μm slices using a rotary microtome cryostat (CryoStar NX50, Leica, USA). The rabbit cornea samples were stained with hematoxylin.

2. Supplementary Figures

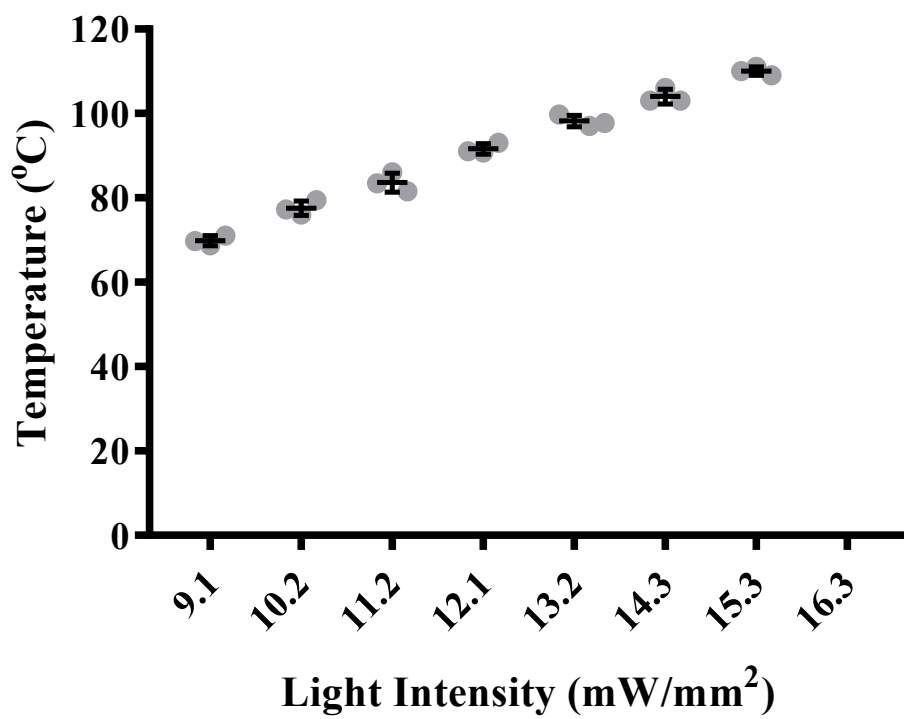


Fig. S1. Equilibrium temperature under different light intensity.

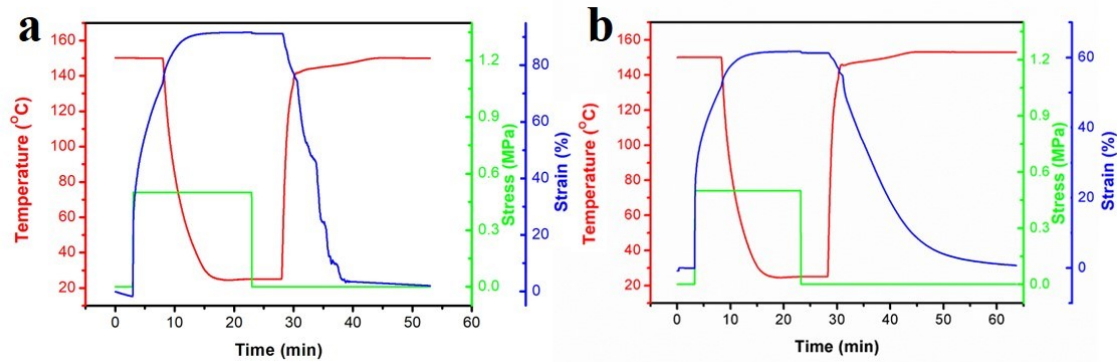


Fig. S2. Shape recovery cycle consisting of a shape-memory creation procedure and recovery under stress-free conditions. (a) pure Nafion Rf: 98.8 %, Rr: 97.7 %, (b) PDA/Nafion composite film Rf: 98.5 %, Rr: 99.2 %.

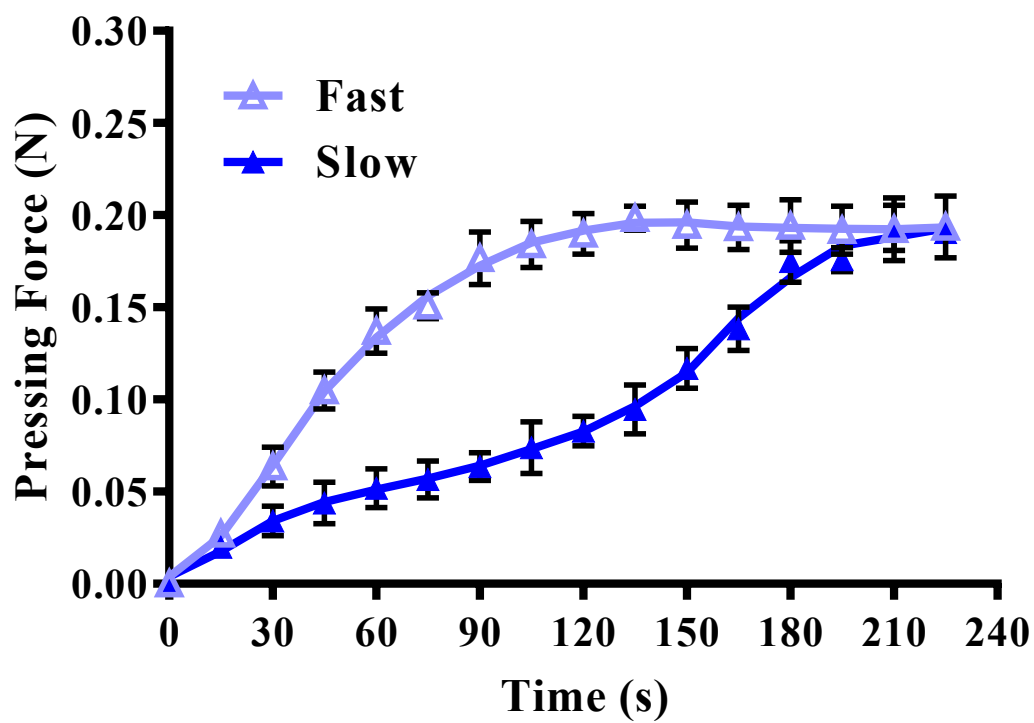


Fig.S3. Pressing force under a fast-heating rate by increasing light intensity to 11.2 mW/mm² within 1s and a slow-heating rate by increasing light intensity to 11.2 mW/mm² within 90s.

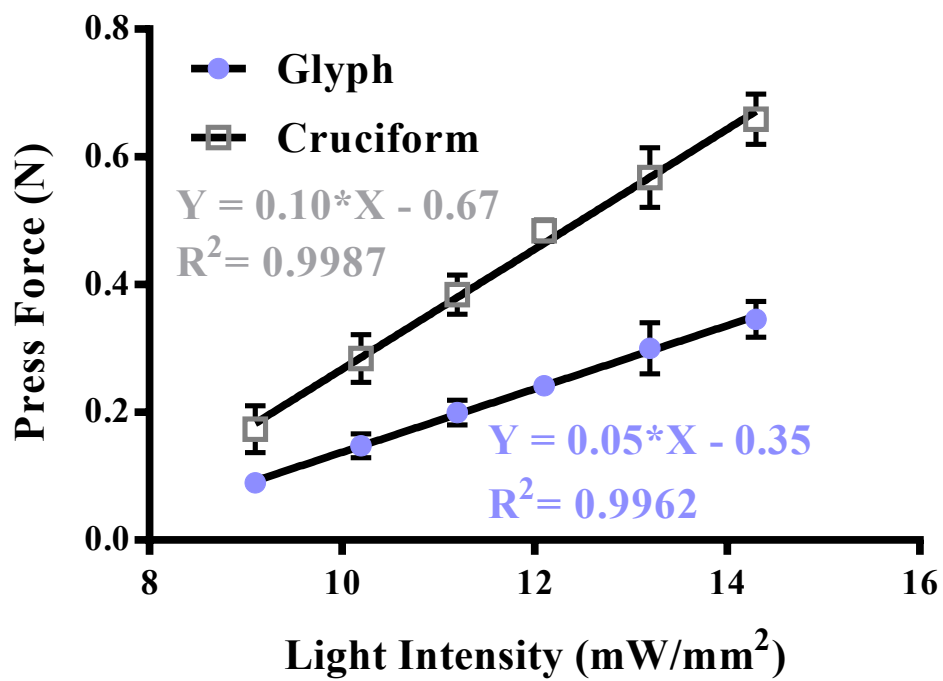


Fig.S4. Plot of the recovery stress versus light intensity for PDA/Nafion composite films with deforming temperature of 100 °C.

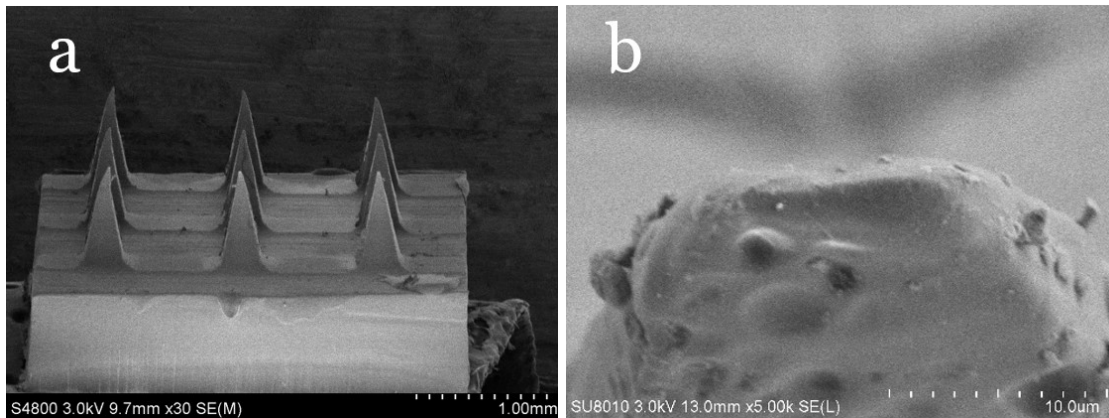


Fig.S5. SEM of (a) PCL MNs and (b) needle tips.

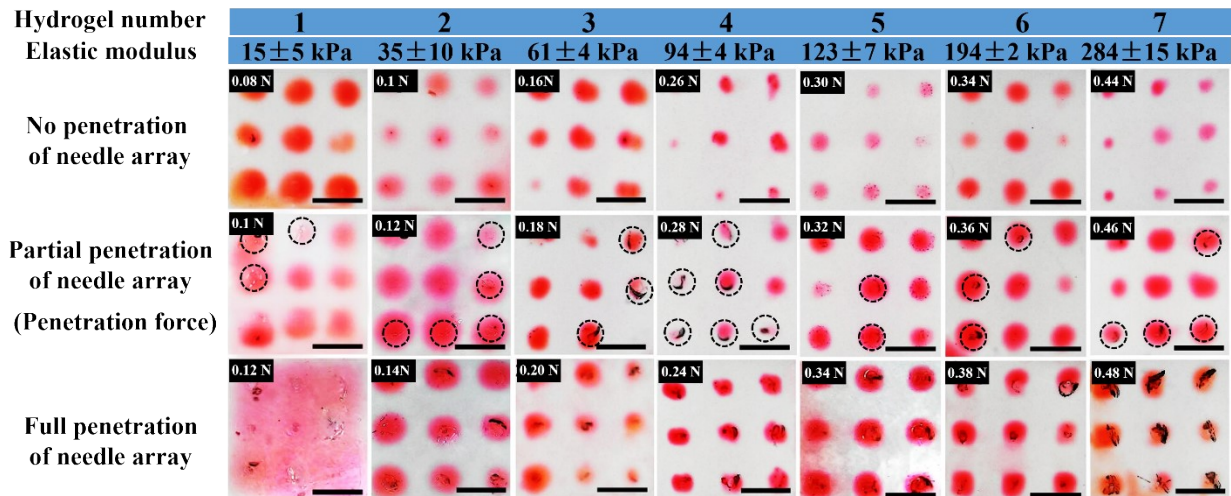


Fig.S6. Representative images of penetration force measurement on phantom tissues. The red dots indicated the diffusion of R6G coated on the MNs (3*3 array). Scale bar: 1 mm.

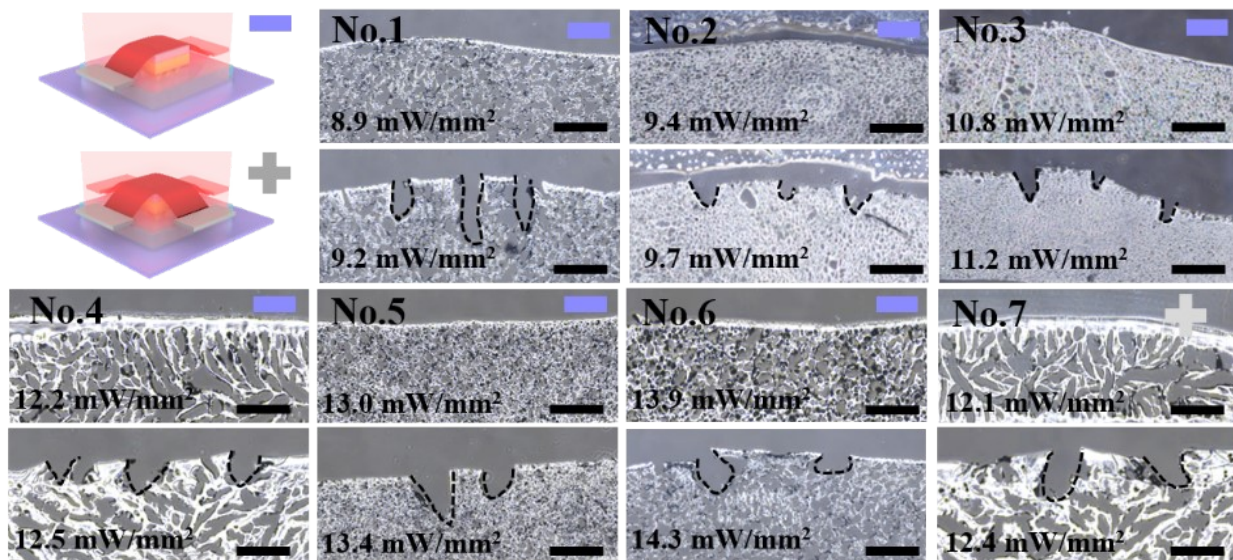


Fig.S7. Penetration on hydrogels using MSPS triggered by NIR light. Strip-shaped MSPS was used in the penetration of No.1-6 phantom tissues, cross-shaped MSPS was used in No.7 phantom tissue. The irradiation intensity was labeled inside. Scale bar: 400 μ m.

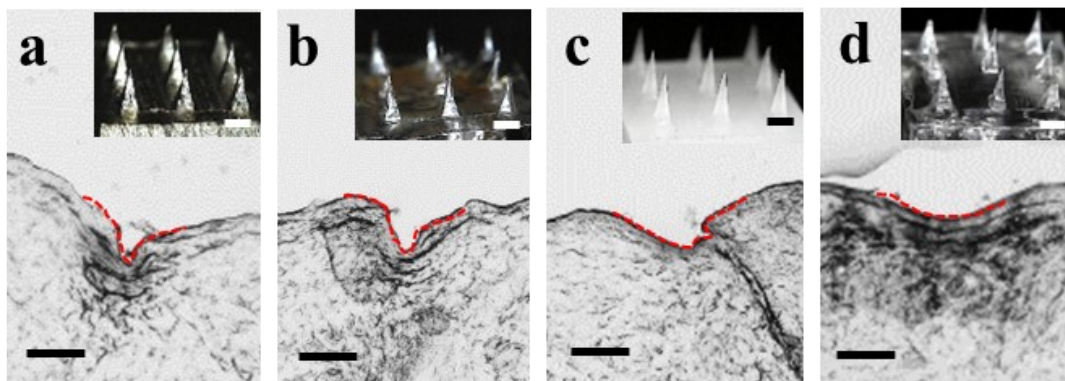


Fig. S8 The histological sections of porcine skin penetrated by cross-shaped MSPS configured with (a) stainless MN, (b) cross-linked chitosan MN, (c) PCL MN, and (d) hyaluronic MN. Scale bar: 300 μ m

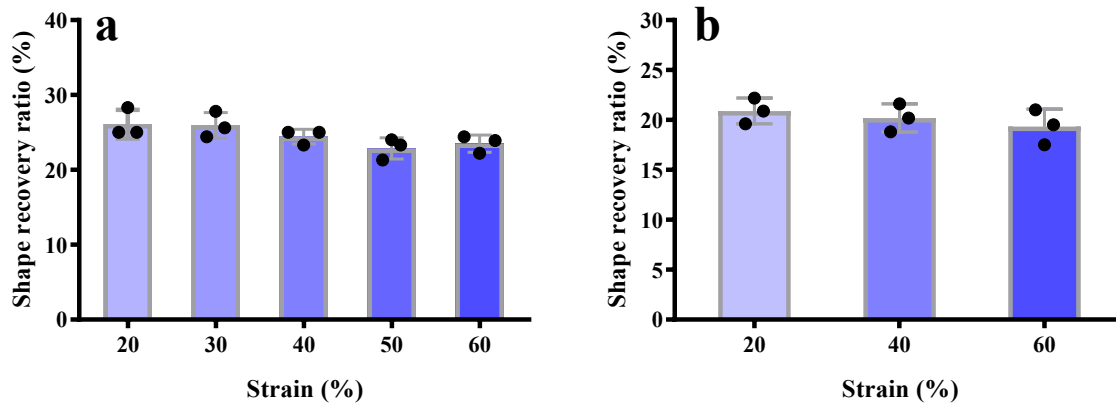


Fig. S9. The shape recovery ratios of different pre-stretch films under the stress of (a) 0.18N and (b) 0.24N.

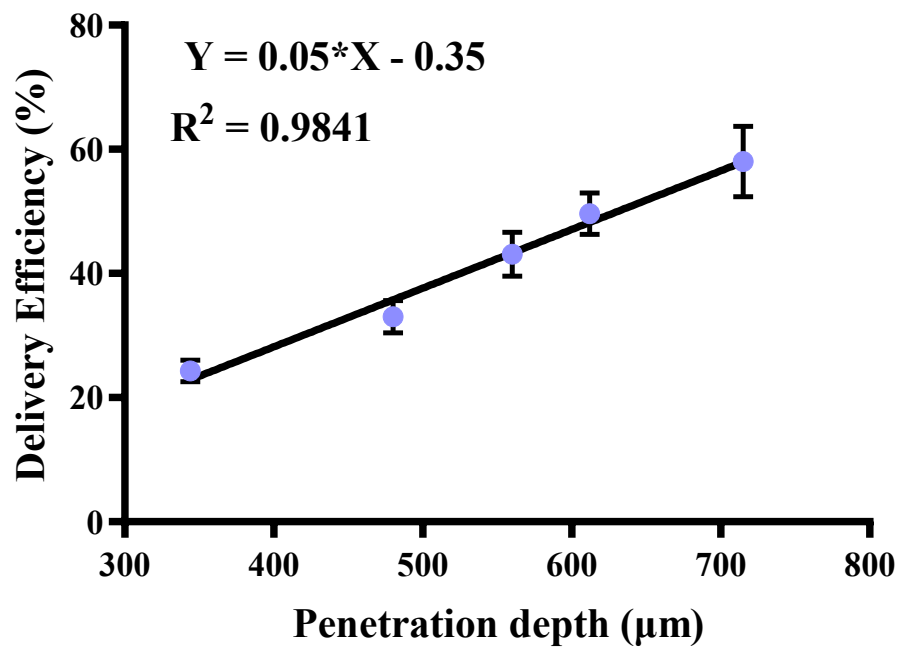


Fig. S10 Drug delivery efficiency at different penetration depth.

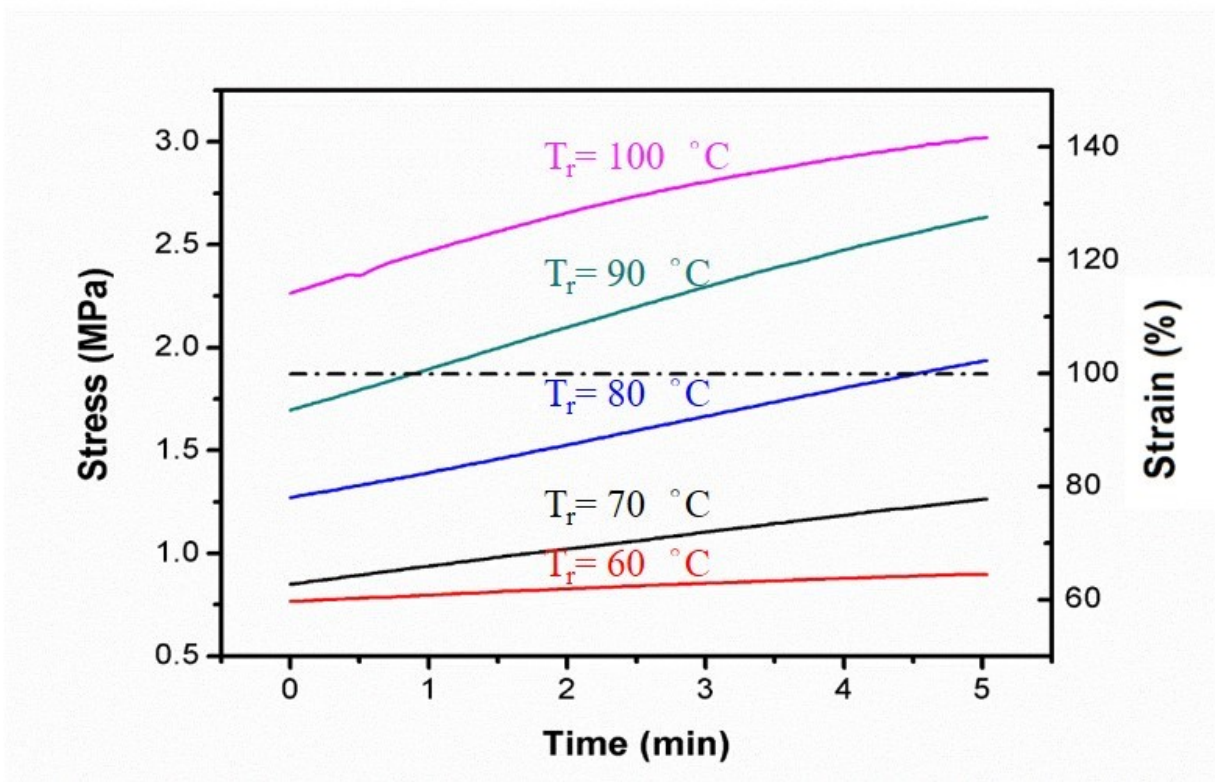


Fig. S11. The relaxation of recovery stress under iso-strain condition ($T_d = 100\text{ }^\circ\text{C}$, strain = 100 %).

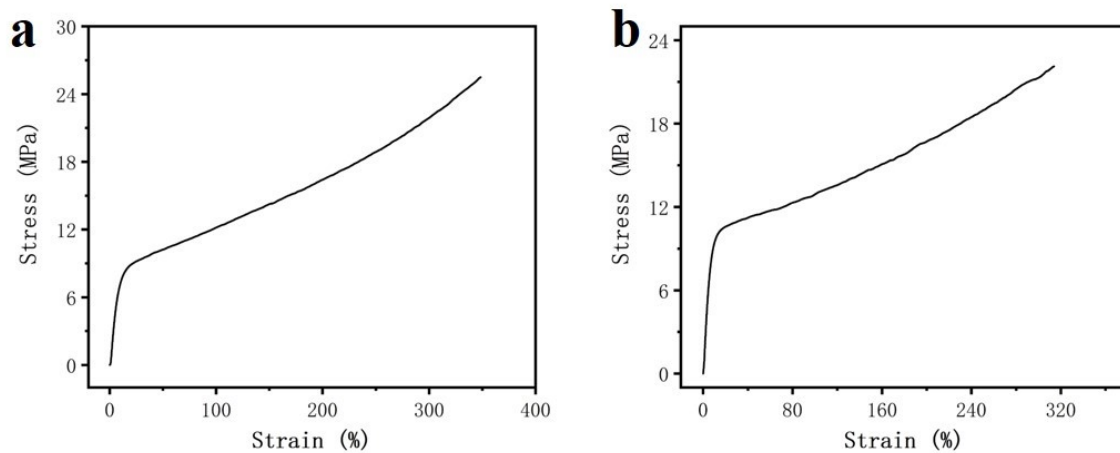


Fig. S12. Elastic modulus and elongation at break of (a) Nafion (elastic modulus =103 MPa, elongation =350 %) and (b) PDA/Nafion (elastic modulus =120 MPa, elongation =320 %).

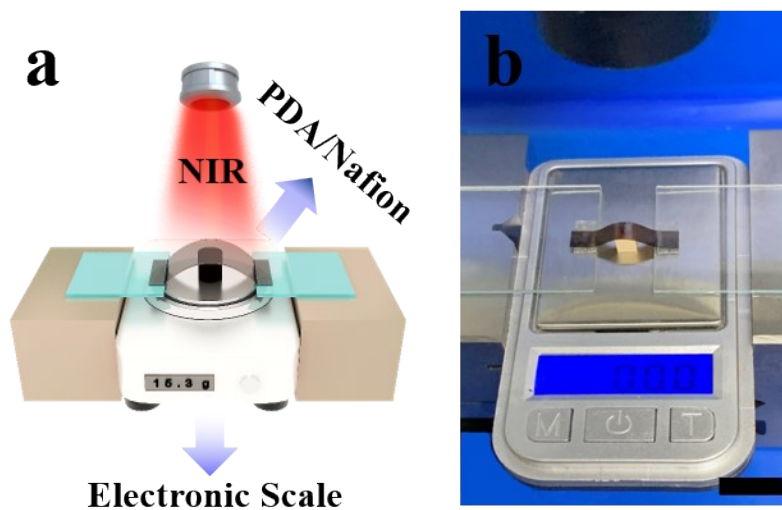


Fig. S13. (a) Schematic and (b) photograph of the stress measurement device. Two glasses were used to tune the distance of the SMP fixed site. A rod was used to regulate the height. The resultant force from the retraction of PDA/Nafion triggered by NIR light could be detected by the electronic scale. Scale bar: 1 cm.

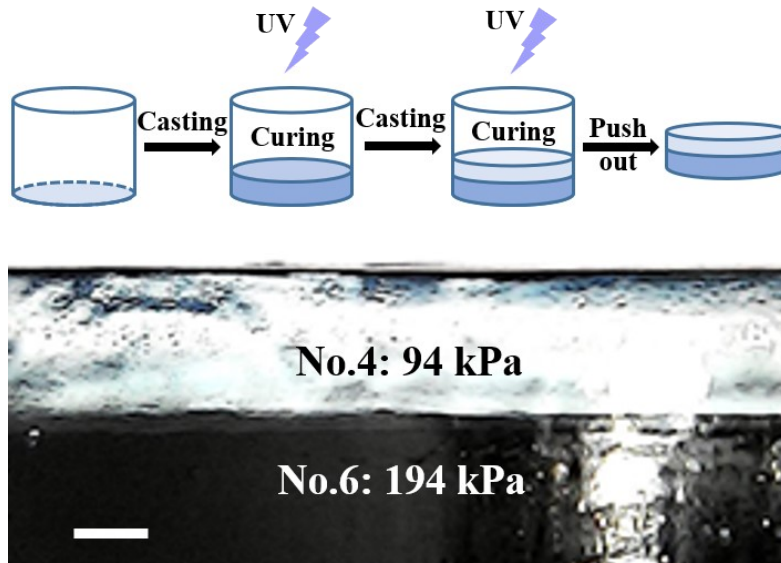


Fig.S14. Fabrication of bilayer phantom tissue. The underlayer (194 kPa) was cured first, and then the precursor solution of the upper layer (94 kPa) was cast on it and cured. After the addition of Methylene blue in the underlayer, the interface between the two layers can be observed. Scale bar: 500 μm .

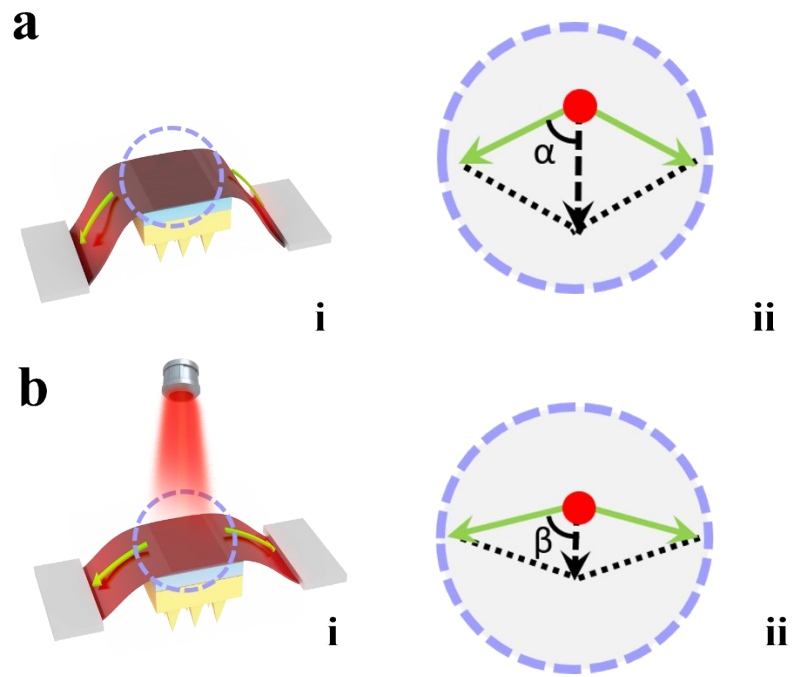


Fig. S15. The stress analysis of the process of penetration.

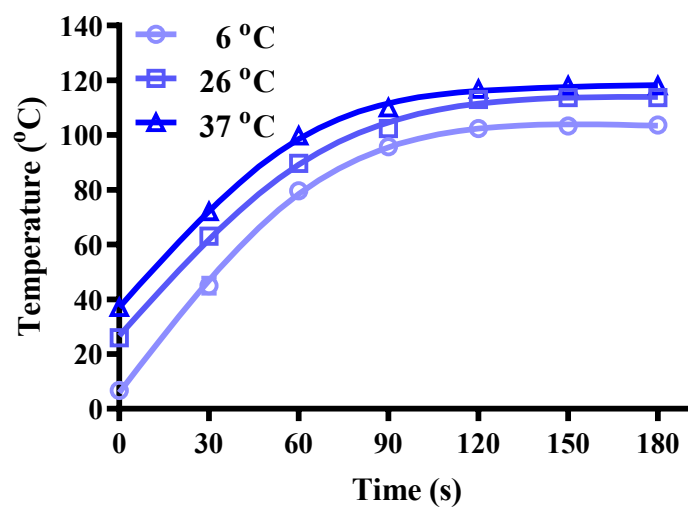


Fig. S16 The photo-thermal conversion temperature as a function of irradiation time at 14.3 mW/mm² under ambient temperature at 6°C, 26°C, and 37°C.

3. Supplementary Tables

Table S1. Regular physical and chemical properties of Nafion and PDA/Nafion

Properties	Nafion	PDA/Nafion
Photo-thermal conversion capacity	none	good
Elastic modulus	103 MPa	120 MPa
Elongation at break	350 %	320 %
R_r (T_d =150 °C, T_r =150 °C)	98.8 %	98.5 %
R_r (T_d =150 °C, T_r =150 °C)	97.7 %	99.2 %
α transition temperature	55 °C-135 °C	40 °C-180 °C
Color	colorless	brown
PDA distribution	/	on the surface and inside of the film

Table S2. The information about pressing force on MN under different NIR irradiation conditions

Intensity Time	9.1 mW/cm²	10.2 mW/cm²	11.2 mW/cm²	12.1 mW/cm²	13.2 mW/cm²
0 s	0	0	0	0	0
30 s	29.15	30.88	34.82	30.95	29.79
60 s	53.11	61.36	74.06	65.69	64.32
90 s	71.89	77.68	93.71	83.64	83.12
120 s	86.92	90.22	109.15	94.69	92.92
150 s	93.91	96.29	104.89	95.30	97.59
180 s	100.00	100.00	100.00	100.00	100.00

Table S3. The information about recovery stress under different intensity of NIR with irradiated time

Hydrogel /Tissue	Components			Elastic modulus (KPa)	Penetration force (N)
	Monomer (w/v %)	Crosslinker (w/w %)	Initiator (w/w %)		
1	10	0.3	0.05	15±5	0.1
2	10	0.6	0.05	35±10	0.12
3	20	0.6	0.05	61±4	0.18
4	20	1.05	0.05	94±4	0.28
5	20	1.25	0.05	123±7	0.32
6	20	1.6	0.05	194±2	0.36
7	20	1.7	0.05	284±15	0.46
Liver				21±10	0.14
Intestinal				32±6	0.16
Stomach				62±6	0.28
Kidney				118±12	0.46
Heart				214±8	0.58
Cornea				447±15	0.74

4. Supplementary Movies

Movie S1. Video of penetration experiment on a bilayer phantom tissue.

Movie S2. Video of penetration experiment using an MSPS configured with SMP of 20% pre-strain.

Movie S3. Video of penetration experiment using an MSPS configured with SMP of 40% pre-strain.

Movie S4. Video of penetration experiment using an MSPS configured with SMP of 60% pre-strain.

Movie S5. Video of penetration experiment in vivo in a rabbit.

Movie S6. Video of patterned insertion of the alphabet "ZJU".

Movie S7. Video of patterned insertion of triangle and square.

References

1. A. K. Denisin and B. L. Pruitt, *ACS Appl Mater Interfaces*, 2016, **8**, 21893-21902.
2. M. Hu, H. Chang, H. Zhang, J. Wang, W. X. Lei, B. C. Li, K. F. Ren and J. Ji, *Adv Healthc Mater*, 2017, **6**, 1601410.